



Chapter 1 Introduction

1.1 Molecular magnets

The discovery of magnetism by humans ^[1] has led to significant advances in modern history. Not only did the invention of the compass allow humans to navigate the globe, but in more recent times the widespread applications of magnetic materials in everyday life, for example in usb sticks, credit cards, computer hard drives and as components in flat screen displays as well as in mobile phones are perhaps little recognized but undoubtedly very important contributions to the modern world. Conventional magnetic materials are two or three dimensional metallic alloys or oxides comprised of transition or/and lanthanide-metal-based spin sites and are typically prepared at high temperature ^[2]. Such materials are so called atomic-based magnets because their active spins are located on the atomic orbitals of corresponded metal ions ^[3]. With the development of the scientific technique, the research area in the field of magnetism gradually shifts from macroscopic to microcosmic.

In the 1950s, Bleaney and Bowers found that the magnetism of Cu^{II} acetate arises from the interaction between two Cu^{II} ions ^[4], resulting in the discovery of molecule-based magnetic coupling. In the 1980s, the discovery of ferromagnetic behavior at 4.8 K in the linear chain electron transfer salt $[\text{FeCp}^*_2][\text{TCNE}]$ (TCNE = tetracyanoethylene) enhanced the belief that ferromagnetism can be achieved using soluble molecules as building blocks ^[5]. This finding led to a new field called molecule-based magnetism ^[6]. Molecule-based magnets are purely organic or inorganic-organic coordination compounds with spins from radicals or metal ions. This type of material can combine magnetic ordering and other properties, such as electrical and optical and can be prepared by conventional organic and inorganic synthetic methodologies at low temperature ^[7].



Chapter 1

Since the discovery of the first molecule-based magnets $[\text{FeCp}^*_2][\text{TCNE}]$ ^[5], many novel molecular magnetic materials varying from zero (0D) to three dimensional (3D) have appeared in the literature ^[8]. These include compounds showing: a) high critical temperature (T_c) magnets; one of the most interesting compound is vanadium tetracyanoethylene $\text{V}(\text{TCNE})_x$, which represents the first molecule-based magnet displaying magnetic order at room temperature ^[9]; b) spin crossover; c) light-tunable magnetism; d) multifunctionality such as magnetic materials also showing chirality, luminescence, ferroelectricity and conductivity.

A further breakthrough for molecular magnets came in 1991 when the first Single Molecule Magnet (SMM) $[\text{Mn}_{12}\text{O}_{12}(\text{OAc})_{16}(\text{H}_2\text{O})_4] \cdot 4\text{H}_2\text{O} \cdot 2\text{AcOH}$ was discovered ^[10]. This molecule shows slow relaxation of magnetization below a certain temperature (so-called blocking temperature) of purely molecular origin. The relaxation between two equally stable ground spin states is blocked by an Energy Barrier which can be related to the uniaxial anisotropy and overall spin of the system ^[10]. Further experiments on the Mn_{12}Ac molecule supported this interpretation through the discovery of stepped hysteresis loops of the magnetization which result from the blocked relaxation as well as quantum tunneling through the energy barrier, occurring as a result of the molecular nature of the compound ^[11]. Such characteristics mean that SMMs have potential application in high-density data storage and quantum computing ^[12].

Compared with traditional magnetic nanoparticles comprised of metals, metal alloys or metal oxides, SMMs have many advantages ^[13]. One of the advantages is their size. SMMs are much smaller than the magnetic nanoparticles using for information storage and each SMM can be viewed as a bit, which might result in the realization of high-density information storage. Furthermore, the peripheral ligands of SMMs can be varied, thus providing a means of tuning the properties of the SMM. Thirdly, SMMs can be soluble in a variety of solvents and this provides



Chapter 1

the opportunity to prepare them as thin films or to attach them to the surface of some substrates, which is important for developing future applications. Finally, whereas traditional magnetic nanoparticles are prepared by a ‘top-down’ approach, SMMs are produced by a ‘bottom-up’ approach. The ‘bottom-up’ approach can give crystalline monodisperse coordination clusters, which can be structurally characterized by single XRD, allowing magneto-structural correlation. Although SMMs present many advantages, the blocking temperatures and energy barrier of SMMs are still very low. Thus, further explorations are necessary for better SMMs.

1.2 Definition of molecular magnetism

1.2.1 Magnetic materials

Paramagnetism results from the intrinsic spin of electrons as well as the motion of the electron constrained within an orbital. There are five classifications of magnetic materials.

a) Diamagnetism: Diamagnetism is an underlying property of matter and it always exists in molecules. This behavior arises from the interactions of paired electrons with the applied magnetic field. Diamagnetic matter is weakly repelled by the applied magnetic field, resulting in negative magnetization.

b) Paramagnetism (Fig. 1.1): This behavior results from the interactions of one or more unpaired electrons with the applied field. Paramagnetic substances are attracted to magnetic field and produce positive magnetization due to alignment of the spins in the direction of the applied field. In the absence of field the spins align randomly, an applied field aligns them and the resulting positive magnetization vanishes when the field is switched off. In other words, there is no magnetic memory effect.

The interactions between paramagnetic atoms or molecule with their surrounding neighbors lead to the properties of bulk magnetic materials.

Chapter 1

c) Ferromagnetism (Fig. 1.1): The spins in ferromagnetic substances interact with each other and are aligned parallel in the same direction, which leads to an increase of the magnetic moment. The magnetic moment can be retained in the absence of magnetic field.

d) Antiferromagnetism (Fig. 1.1): The spins in an antiferromagnetic material interact with each other such that there is an antiparallel alignment resulting in a zero magnetic moment.

e) Ferrimagnetism (Fig. 1.1): Ferrimagnetism is a special case of antiferromagnetism. The arrangement of the spins in ferrimagnetic substance is still antiparallel, but there is incomplete cancellation of the spins, leading to an overall magnetic moment ^[14].

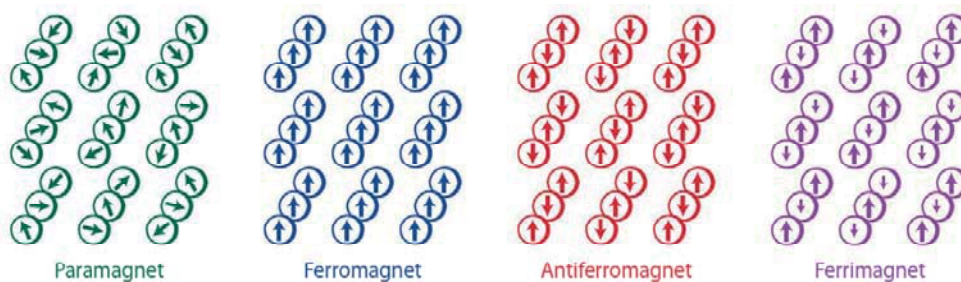


Fig. 1.1 The alignments of magnetic moment for paramagnetic, ferromagnetic, antiferromagnetic and ferrimagnetic material ^[14b].

1.2.2 The description of the magnetic behavior

Susceptibility: Magnetic susceptibility (χ) is the quantitative measurement of the response of a material to an applied field, which is defined as

$$\chi = \frac{dM}{dH} \quad \text{Equation 1}$$



Chapter 1

where M is magnetization and H is applied magnetic field. When the applied field H is weak enough, χ is independent of H , such that the equation above can be written as

$$\chi = \frac{M}{H} \quad \text{Equation 2}$$

In principle, χ is the sum of diamagnetic (χ^D) and paramagnetic (χ^P) susceptibility

$$\chi = \chi^D + \chi^P \quad \text{Equation 3}$$

The former is negative and the latter is positive. Diamagnetism is the fundamental property of matter. It always exists, even when it is masked by the paramagnetism. χ^D is temperature and field independent and its value can be estimated by empirical methods using Pascal's constants or the molecular weight of the measured compound ^[15a]

$$\chi^D = (0.4 \sim 0.5) \times MW \times 10^{-6} \text{ cm}^3 \text{ mol}^{-1} \quad \text{Equation 4}$$

where MW is the molecular weight.

Magnetic interactions are generally determined by their response to variation of temperature and applied magnetic field. The temperature dependent susceptibility measurements can often be described using a Curie-Weiss law, whereas the field dependent magnetization measurements may be fit using a Brillouin function.

Curie-Weiss law: For paramagnetic materials with isolated spin sites, the relation between susceptibility and temperature can be described by the Curie law:

$$\chi = \frac{C}{T} \quad \text{Equation 5}$$

where C is Curie constant and T is absolute temperature. The Curie law is valid when there are no interactions between the neighboring spins. When there are couplings between spins, the magnetic behavior can be modeled as a function of temperature by Curie-Weiss law:

$$\chi = \frac{C}{T - \theta} \quad \text{Equation 6}$$

where θ is the Weiss constant. The Curie constant (C) and Weiss constant (θ) can be deduced from the χ^{-1} versus T plots. The combination of Weiss constant (θ) and χT versus T plots can be used to classify the nature of the magnetic behavior (Fig. 1.2). For paramagnetism, $\theta = 0$ and the χT versus T curve presents a horizontal line. For ferromagnetism, $\theta > 0$ and the χT product increases with decreasing temperature. For antiferromagnetism, $\theta < 0$ and the χT product decreases with decreasing temperature. For ferrimagnetism, $\theta < 0$ and the χT product decreases with decreasing temperature to a minimum and then increases suddenly on lowering the temperature.

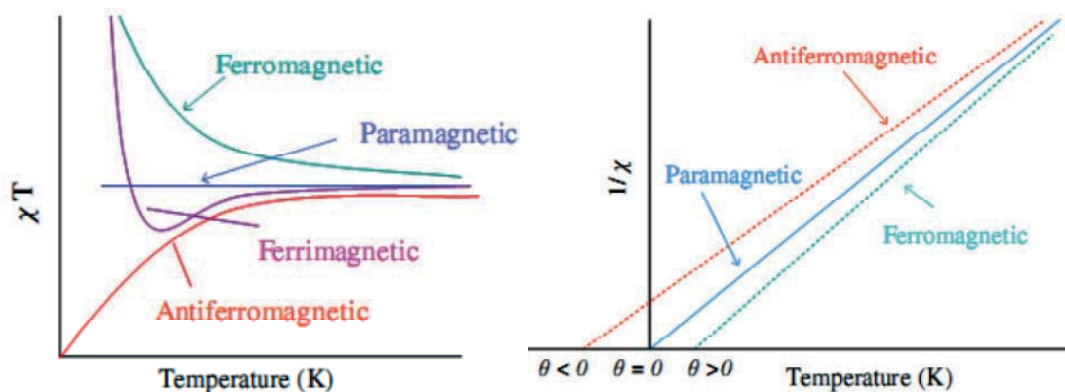


Fig 1.2 The χT vs T (left) and χ^{-1} vs T (right) plots for paramagnetic, ferromagnetic, antiferromagnetic and ferromagnetic material ^[15b].

Brillouin function: For paramagnetic substances with non-interacting spins, the magnetization as a function of applied magnetic field can be calculated using a Brillouin function:

$$M = gSN\beta B_S \quad \text{Equation 7}$$

$$B_S(y) = \frac{2S + 1}{2S} \coth\left(\frac{2S + 1}{2S} y\right) - \frac{1}{2S} \coth\left(\frac{1}{2S} y\right) \quad \text{Equation 8}$$

Chapter 1

$$y = \frac{gS\beta H}{kT} \quad \text{Equation 9}$$

where g is the Landé factor, S the total spin, N is the Avogadro's number, $N\beta$ is the Bohr magneton, k is the Boltzmann constant. When $y \gg 1$, H/kT is very large, then $B_S(y) = 1$ and M tends to the saturation value M_s :

$$M_s = gSN\beta \quad \text{Equation 10}$$

From this equation, the ground spin state of a material can be evaluated without knowing the chemical components of the material.

When $y \ll 1$, H/kT very small,

$$B_S(y) = \frac{S+1}{3S} y \quad \text{Equation 11}$$

Since $\chi = M/H$, the following equation can be written:

$$\chi = \frac{M}{H} = \frac{Ng^2\beta^2}{3kT} S(S+1) = \frac{C}{T} \quad \text{Equation 12}$$

The above equation is the Curie law, which is valid for the spin-only system^[15]. The plots of M in $N\beta$ units for $g = 2$ versus H/T for different S are shown in Fig. 1.3.

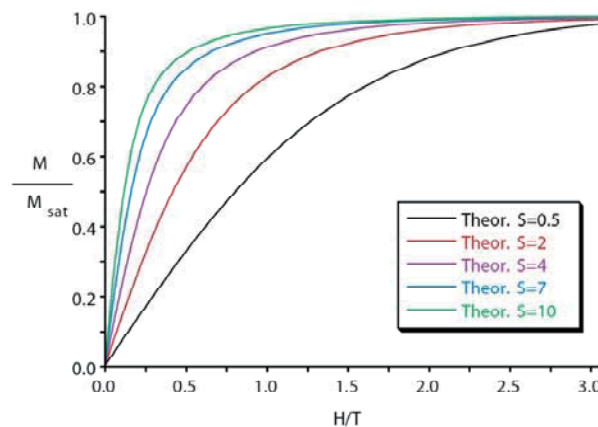


Fig. 1.3 Plots of magnetization normalized to the saturation magnetization versus H/T for different S values^[14b].

1.3 Single molecule magnets

SMMs are a class of discrete metal-organic compounds, which can be designated as coordination clusters and which show slow relaxation of magnetization or/and magnetic hysteresis loops at low temperature ^[10-11]. For a cluster with $S > 1/2$ systems, S can be split into $2S+1$ microstates (corresponding to the M_s states) by spin-orbit coupling or magnetodipolar interactions in zero field (Fig. 1.4). This results from zero-field splitting (ZFS) ^[16] where a uniaxial anisotropy can be quantified by the parameter D . The anisotropy removes the degeneracy and locates the highest magnitude levels ($M_s = \pm S$) into the places with lowest energy (Fig. 1.4). In order to reorient the magnetization, an energy barrier (ΔE) between $M_s = -S$ and $M_s = 0$ should be overcome, which is defined as

$$\Delta E = |D|S^2 \quad \text{Equation 13}$$

for integer spin states or

$$\Delta E = |D| \left(S^2 - \frac{1}{4} \right) \quad \text{Equation 14}$$

for half-integer spin states. In the frame of this description, the D value should be negative to allow the maximum absolute value of the spin ground state to be lowest in energy, thereby producing a barrier to spin inversion between the + and – ground states ^[17a].

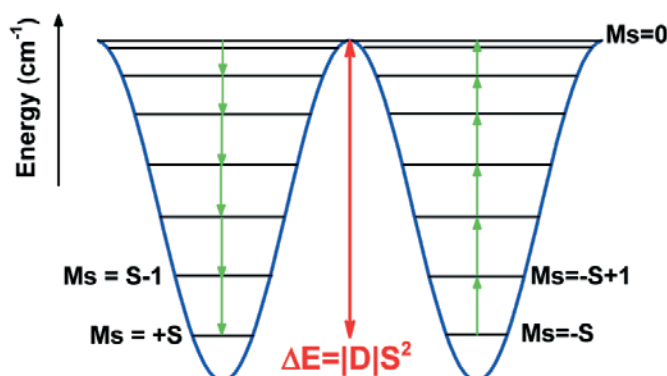


Fig. 1.4 Energy levels for a spin state S with easy axis magnetic anisotropy.



Chapter 1

The relaxation process of a SMM can be detected using alternating current (ac) susceptibility measurements. Generally, on the standard SQUID-based magnetometers available the ac susceptibility measurements are carried out between 1.5 and 50 K (for most SMMs) varying the frequency from 1-1500 Hz using a small oscillating ac field between 1-5 Oe. The measurements can be performed with or without the presence of a direct current (dc) magnetic field. The rationale can be described as follows.

Each SMM molecule has its own magnetic moment, so the magnetization of the SMM will lag behind the driving ac field when it passes through the sample, thus the measured magnetic susceptibility will produce a phase shift. The signals collected from this experiment can be split into in-phase and out-of-phase susceptibilities, respectively, in terms of the fundamental response of magnetic materials with electromagnetic radiation. Thus an important aid to observe SMM behavior is to study the variation of in-phase and out-of-phase signals with temperature at different frequencies or with frequency at different temperatures.

When the curves of the out-of-phase signals give peaks and the peaks shift to high temperature with increasing frequency (Fig. 1.5), this indicates that the magnetization of SMM has been reoriented^[17].

Furthermore, we can inspect the SMM behavior by plotting the ac signals with frequency at different temperature (Fig. 1.6). If peaks show up in the curves of out-of-phase signals and the maxima move to higher frequency with increasing temperature, it suggests SMM behavior. The relaxation time and energy barrier can be extracted from the frequency-dependent plots. This is the most popular ways to get these two parameters. Each frequency-dependent plot gives a relaxation time (τ) at a certain temperature (T), and the relationship between τ and T is determined by Arrhenius law

Chapter 1

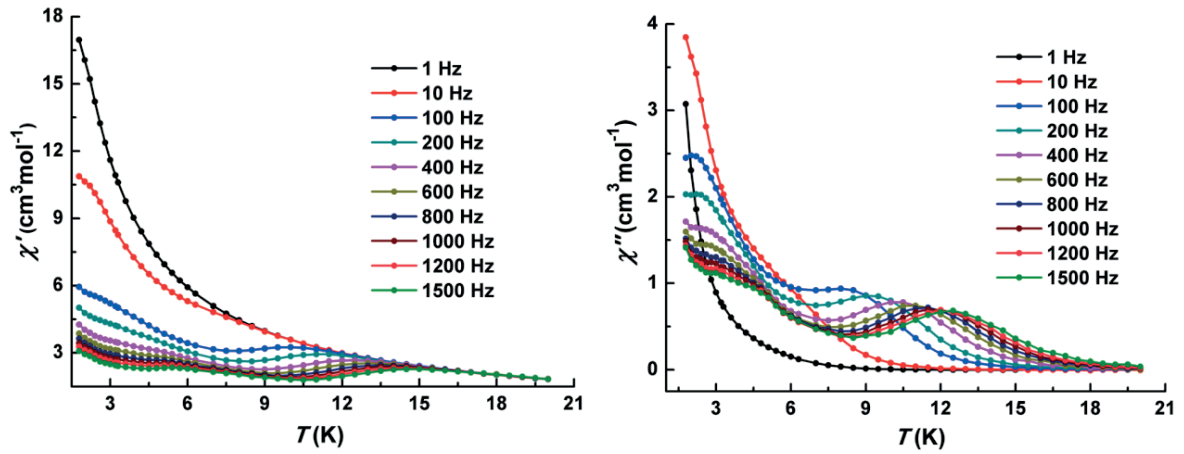


Fig. 1.5 Temperature dependence of in-phase (left) and out-of-phase (right) ac magnetic susceptibility for a SMM.

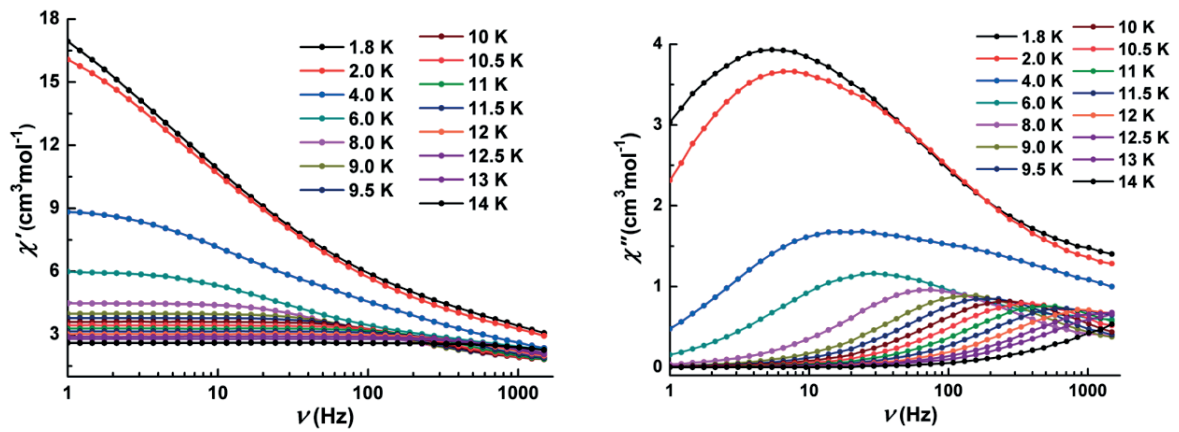


Fig. 1.6 Frequency dependence of in-phase (left) and out-of-phase (right) ac magnetic susceptibility for a SMM.

$$\tau = \tau_0 \exp\left(\frac{\Delta E}{kT}\right) \quad \text{Equation 15}$$

The energy barrier and relaxation time can be evaluated from the slope and intercept of $\ln\tau$ versus $1/T$ curve, which is a linear and the $\ln\tau$ is temperature dependent.

$$\ln\tau = \frac{\Delta E}{kT} + \ln\tau_0 \quad \text{Equation 16}$$

Chapter 1

If the conditions mentioned above are satisfied, the magnetization of the SMM is said to relax through a thermally assisted process ^[17b].

Another character of SMMs is the presence of magnetization versus field hysteresis loops at low temperature. In general hysteresis loops differ varying from macroscopic to nanoscopic systems (Fig. 1.7) ^[17a, 18]. The steps in the loops for a SMM are ascribed to quantum tunneling of the magnetization (QTM) (Fig. 1.7, right). QTM results from transverse anisotropy which gives a superposition of the M_s microstates on both sides of the barrier *via* tunneling. QTM only can happen when the two M_s microstates on either side of energy barrier have similar energy. The hysteresis can be observed by the micro-SQUID technique ^[18]. If the hysteresis loops increase with decreasing temperature and increasing field sweep rates, this indicates the reversal of the magnetization.

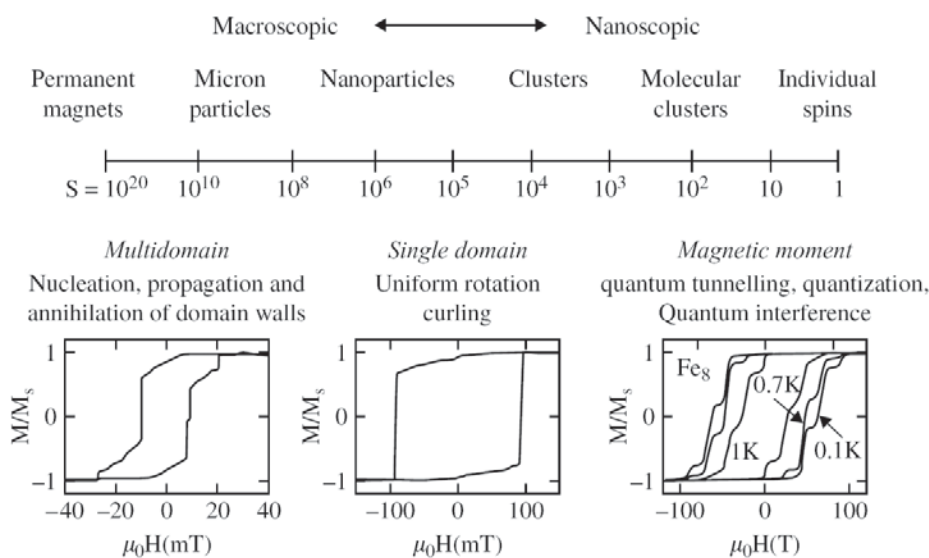


Fig. 1.7 The hysteresis loops from macroscopic to nanoscopic (from left to right) ^[17a].

Sometimes QTM also can be observed in Arrhenius plots. In general, an Arrhenius plot should be linearly temperature-dependent. However, at low



temperatures the plots can present a series of consecutive data points for which the $\ln\tau$ is temperature independent and this indicates the so-called quantum region ^[17c]. Thus the plot displays both temperature-dependent linearity at high temperature and a quantum region at low temperature at the same time suggesting the relaxation process of SMM occurs by mixing thermal and QTM mechanisms ^[17b].

In summary, a SMM is a discrete coordination cluster that shows slow relaxation of magnetization of purely molecular origin. The slow relaxation of the magnetization results from the combination of large spin ground state (S) and negative anisotropy (D). The relaxation can occur via thermal, QTM or mix thermal and QTM mechanisms. These relaxation processes can be observed by ac susceptibility or micro-SQUID measurements.

1.4 Fe^{III}-Ln^{III} SMMs

The relaxation of SMMs strongly depends on the spin ground state (S) and magnetic anisotropy (D), the combination of these two parameters gives an energy barrier to reorient the magnetization, which has been discussed in the last section. Since the discovery of the first SMM Mn₁₂-ac ^[10], many efforts have been devoted to the synthesis of transition metal (3d) SMMs ^[19-20]. However, it was found that increasing the nuclearity, to enlarge the spin values might not be the best strategy to improve SMM behavior. Recently, attention has been focused on the design of SMMs containing lanthanide (4f) metal ions because of the large magnetic anisotropy resulting from unquenched orbital angular momentum of 4f metal ions and many 4f ^[17b, 21] and 3d-4f SMMs ^[22-27] have been reported.

As one subfield of 3d-4f coordination chemistry, Fe^{III}-Ln^{III} coordination clusters are fascinating. Firstly, Fe^{III} can offer higher spin ground state ($S = 5/2$) compared with other transition metal ions and the Fe^{III}-Fe^{III} interactions are strong. Secondly, the Ln^{III} not only can contribute up to seven unpaired 4f electrons to the

total spin, but also present large magnetic anisotropy resulting from unquenched orbital angular momentum. Thus, the combination of these two advantages mentioned above in one compound might increase the possibilities to obtain SMMs with improved properties. Based on this strategy, some $\text{Fe}^{\text{III}}\text{-Ln}^{\text{III}}$ SMMs have been reported [28]. For example, the first ferromagnetically coupled $\text{Fe}^{\text{III}}_4\text{Dy}^{\text{III}}_4$ compound has been reported by Powell *et al.* This compound displays SMM behavior below 4 K with an energy barrier of 30.5 K (Fig. 1.8). In 2013, a nonanuclear $\text{Fe}^{\text{III}}_6\text{Dy}^{\text{III}}_3$ coordination cluster with highest energy barrier of 65.1 K for $\text{Fe}^{\text{III}}\text{-Ln}^{\text{III}}$ system has been reported by the same group (Fig. 1.9, left). Bu *et al.* reported the first $\text{Fe}^{\text{III}}\text{-Sm}^{\text{III}}$ SMM $\text{Fe}^{\text{III}}_{12}\text{Sm}^{\text{III}}_4$, which shows relaxation below 3 K with an energy barrier of 16 K (Fig. 1.9, right).

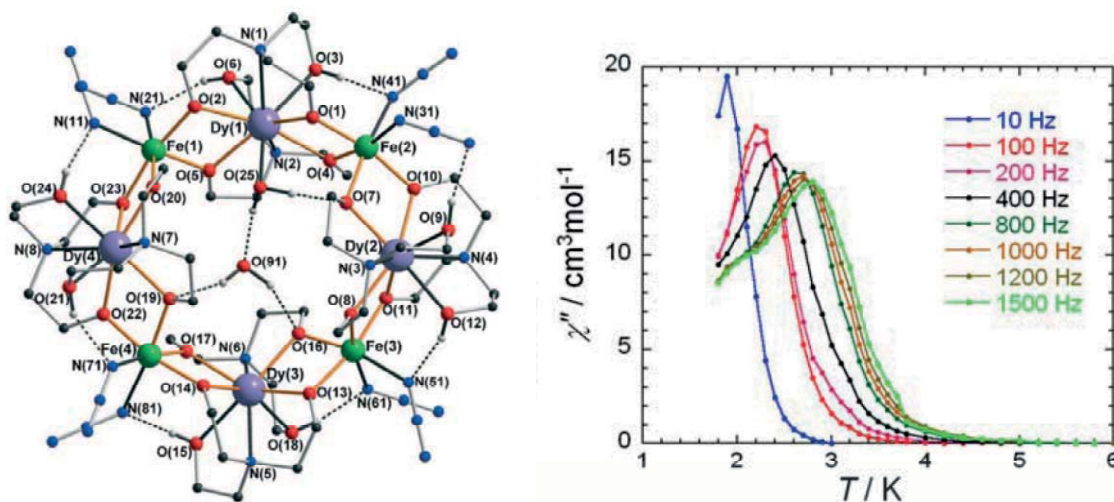


Fig. 1.8 The structure (left) and out-of-phase ac susceptibility (right) for $\text{Fe}^{\text{III}}_4\text{Dy}^{\text{III}}_4$.

However, the literature survey shows the blocking temperature and energy barrier for $\text{Fe}^{\text{III}}\text{-Ln}^{\text{III}}$ SMMs are still very low, so there is a continuing need for the synthesis and characterization of new $\text{Fe}^{\text{III}}\text{-Ln}^{\text{III}}$ coordination clusters to increase the knowledge and improve the properties of $\text{Fe}^{\text{III}}\text{-Ln}^{\text{III}}$ SMMs.

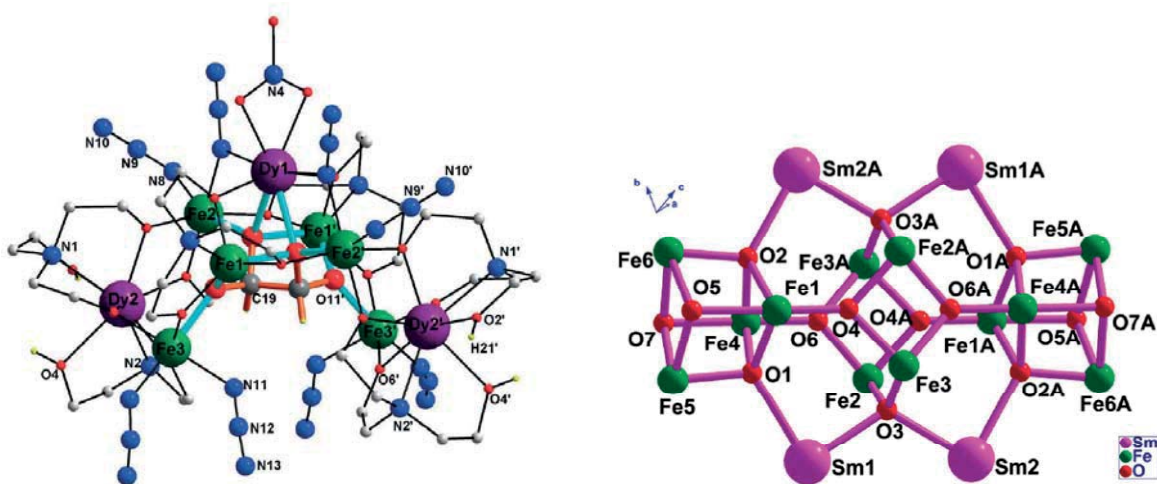


Fig 1.9 The structure of $\text{Fe}^{\text{III}}_6\text{Dy}^{\text{III}}_3$ (left) and the core of $\text{Fe}^{\text{III}}_{12}\text{Sm}^{\text{III}}_4$ (right).

1.5 ^{57}Fe Mössbauer spectroscopy

1.5.1 Fundamental of Mössbauer spectroscopy

For a free nucleus, when a γ ray is emitted after a nuclear transition, it recoils due to the conservation of momentum. This means that the emitted γ ray has less energy than the resonant line. Conversely, more energy is needed than the resonant line in order to excite a nucleus. This leads to a displacement between the centers of emission and absorption lines by twice the recoil energy of the nucleus. The displacement is much larger than the natural width of most γ rays and the Doppler width (width of spectral lines due to the Doppler effect caused by a distribution of velocities of atoms or molecules). Thus the energy resolution of recoil transitions is low, which is not suitable for practical exploration ^[29].

When the emitting and absorbing nuclei are in a solid matrix, the effective mass of the nucleus becomes much greater. The recoiling mass now corresponds to the mass of the whole system, making the recoil energy very small. If the recoil energy is smaller than the energy of a phonon (lattice vibrational energy), recoilless emission and resonance absorption occur. This is the Mössbauer effect. This phenomenon was discovered by Rudolph Mössbauer who received the Noble Prize



Chapter 1

in 1961 for his work. The recoilless transitions reduce the recoil energy and Doppler width, which makes Mössbauer spectroscopy a very sensitive technique to probe the hyperfine interactions of an atomic nucleus and its environment ^[30].

In order to detect the intensity of the resonant absorption, the emission energy of γ rays must be varied continuously over a small range. This modulation can be achieved by employing the Doppler effect resulting from the movement of the source and the absorber.

$$E_{\gamma} = E_0 \left(1 \pm \frac{v}{c} \right) \quad \text{Equation 17}$$

where v is the relative velocity of source and absorber, c is the velocity of light ^[31]. Therefore, the resulting spectrum is the plot of the rate of transmission of the γ ray through the absorber as a function of velocity. The number, positions and intensities of the peaks in the spectra provide precious information about the nucleus and its environment ^[32].

1.5.2 Mössbauer parameters

Isomer shift (δ): The isomer shift results from the difference in the electron densities at the nuclear sites in the emitting and absorbing atoms. The difference in density changes the Mössbauer transition energy and the Mössbauer spectrum is shifted (Fig. 1.10, left). Isomer shift values can give information about oxidation state, spin state, and bonding properties such as covalency of coordination compounds and electronegativity of the ligand ^[33, 34]. Fig. 1.10 gives an overview of the isomer shift of different iron complexes with various oxidation states ^[31].

Quadrupole Splitting (ΔE_Q): If the investigated nuclei do not have a charge distribution that is spherically symmetric then they will possess an electric nuclear quadrupole moment. This moment interacts with an asymmetric electronic charge distribution to give a quadrupole splitting, Δ , of nuclear energy levels. For example ⁵⁷Fe has $I = 3/2$ and leads to two states $m_I = 1/2$ and $m_I = 3/2$ resulting in a two line